PAIN®

Targeting brain-derived neurotrophic factor in the medial thalamus for the treatment of central poststroke pain in a rodent model

Hsi-Chien Shih, Yung-Hui Kuan, Bai-Chung Shyu*

Abstract

Approximately 7% to 10% of patients develop a chronic pain syndrome after stroke. This chronic pain condition is called central poststroke pain (CPSP). Recent studies have observed an abnormal increase in the secretion of brain-derived neurotrophic factor (BDNF) in spinal cord tissue after spinal cord injury. An animal model of CPSP was established by an intrathalamus injection of collagenase. Mechanical and thermal allodynia was induced after lesions of the thalamic ventral basal complex in rats. Four weeks after the injection, the number of neurons decreased, the number of astrocytes, microglia, and P2X4 receptors increased, and BDNF mRNA expression increased in the brain lesion area. Nociceptive activity in the medial thalamus (MT) and the coherence coefficient of spontaneous field potential oscillations in the anterior cingulate cortex were enhanced in CPSP animals, and these enhancements were blocked by an acute injection of TrkB-Fc and TrkB antagonist Tat Cyclotraxin-B. Instead of being inhibited by the γ-aminobutyric acid (GABA) system in normal rats, multiunit activity in the MT was enhanced after a microinjection of muscimol, a GABA$_A$ receptor agonist, in CPSP animals. After CPSP, BDNF expression was enhanced in the MT, whereas the expression of GABA$_A$ channels and the cotransporter KCC2 decreased in the same area. These findings suggest that neuronal plasticity in the MT that was induced by BDNF overexpression after the thalamic lesion was a key factor in CPSP.

Keywords: Central post stroke pain, Central neuropathic pain, Brain-derived neurotrophic factor, Medial thalamus, Anterior cingulate cortex

1. Introduction

Stroke continues to be a concern in modern society, the incidence of which is growing among the aging population. Although the incidence of hemorrhagic stroke is less than ischemic stroke,[9] the rate of mortality that is associated with hemorrhagic stroke is higher than ischemic stroke.[30] In addition to functional losses in motor function and cognition that follow stroke, approximately 8% to 14% of stroke survivors with hemorrhagic damage in lateral thalamic regions suffer abnormal central poststroke pain (CPSP). These patients suffer from allodynia and hyperalgesia after stroke, which are among the most troublesome sequelae of stroke.[24] Central poststroke pain is a neuropathic pain syndrome that is associated with somatosensory abnormalities after stroke. Because of potential underdiagnosis and difficulty in managing the condition, previous studies have been unable to clearly establish the detailed mechanisms of CPSP, and therapies are limited.[1,25]

Neuroinflammation is believed to be an important factor in the induction of chronic pain.[28,32] Some studies suggest that neurogenic pain syndromes can be effectively relieved by inhibiting neuroinflammatory processes.[17,31,42] We recently found that P2X7 receptors are involved in neuronal hypersensitivity associated with CPSP.[23] However, additional posttraumatic processes may also be involved in the pathophysiology of CPSP. The overexpression of brain-derived neurotrophic factor (BDNF) by proliferating microglia or glia after injury is another key factor that is related to neuropathic pain.[4,39] Expression of the K-Cl cotransporter KCC2 and Na-K-Cl cotransporter NKCC1 in mature neurons is altered by BDNF overexpression, which can cause abnormal neuronal excitation.[5,19] Although BDNF overexpression is involved in neuropathic pain, it is still unclear whether these factors also mediate persistent pain in CPSP.

In this study, we hypothesized that persistent CPSP is caused by BDNF overexpression after brain tissue damage. The blockade of BDNF cascades after stroke can alter central pain conditions. The aim of this study was to assess posttraumatic processes and the neuromodulatory effects of BDNF on neuronal sensitivity and nociceptive behavior in a rat model of CPSP. Our data demonstrate that the noxious response and oscillation pattern of the thalamocortical pathway are altered in CPSP rats. Both neuronal noxious responses and allodynia behavior in rats after CPSP were reversed to a normal state by TrkB-Fc and Tat Cyclotraxin-B treatment. We also found that thalamic neurons were excited by a γ-aminobutyric acid-A (GABA$_A$) receptor agonist in CPSP rats. The decrease in the

cotransporter KCC2 and increase of phosphorylated KCC2 at Ser940 residue (pS940-KCC2) may be caused by BDNF over-expression and contribute to the reversal of GABAergic function.

2. Materials and methods

2.1. Preparation of central poststroke pain animal model

Adult male Sprague Dawley rats (300-400 g; BioLASCO, Taipei, Taiwan) were housed in independent ventilation cages with free access to food and water. All the experiments were performed in accordance with the guidelines of the Academia Sinica Institutional Animal Care and Utilization Committee. The experimental rats were randomly selected and blindly tested during each session to avoid any anticipatory effects. The lesion protocols were modified from our previously described procedures.[22,27,36] During surgery, the animals were maintained under anesthesia with 1% to 2% isoflurane. Animal body temperature was maintained at 36.5 to 37.5°C with a homeothermic blanket system (Model 50-7079; Harvard Apparatus, Holliston, MA). To induce the hemorrhagic lesion, the animals were injected with type IV collagenase (0.125 U/0.5 μL saline; C5138, Sigma, St. Louis, MO) in the right ventrobasal (VB) complex of the thalamus (coordinates: 3.0-3.5 mm posterior, 3.0-3.4 mm lateral to bregma, 5.7-6.0 mm depth). Sham control animals were injected with 0.5 μL saline only. The experimental rats were given 3 mg gentamicin intraperitoneally every day for 5 days after each surgical procedure. For the in vivo acute electrophysiological recording groups, the rats received an acute microinjection of artificial cerebrospinal fluid (1 μL/min), denatured TrkB-Fc (dTrkB-Fc, 1 μg/μL/min; Sigma), TrkB-Fc (1 μg/μL/min; Sigma), or muscimol (15 μM/μL/min, Tocris, Bristol, United Kingdom) with a 30-gauge stainless-steel cannula in the medial thalamus ([MT]; 2.5 mm posterior, 1.5 mm lateral to bregma, 4.2 mm depth) under isoflurane anesthesia. For the group of rats that received chronic microinjections under awake conditions, a 27-gauge stainless-steel cannula was implanted in the VB (2.5 mm posterior, 2.5 mm lateral to bregma, 5.2 mm depth) and conglutinated with dental resin under the same anesthetic procedure. On day 36, dTrkB-Fc, TrkB-Fc (1 μg/μL/d), or Tat cyclotraxin-B (CTX-B; 0.5 μL of solution, 10 μg/μL/d, Tocris, Bristol, United Kingdom) was applied at a rate of 0.3 μL/min per injection using a 30-gauge stainless-steel cannula in the VB once per day followed by a 5-day rest period (days 36-40).

2.2. Behavioral testing

2.2.1. von Frey test

The rats were habituated for 30 minutes before testing. Von Frey filaments were gradually applied with ascending, graded force to determine the minimal force that elicited a limb withdrawal response. The threshold was defined as the average of 3 minimal forces measured in consecutive trials, with a 5-minute intertrial interval.

2.2.2. Plantar test

The rats were habituated to a transparent Plexiglas box for 30 minutes before testing. The plantar test was performed by radiant heating (IITC 390 G Plantar Test; IITC Life Science, Woodland Hills, CA). The hind paw was stimulated by an infrared light beam source to elicit noxious withdrawal responses. The paw withdrawal latency in response to infrared light stimulation was measured. Each rat was tested in 3 trials with the right and left hind paws, respectively, with a 5-min intertrial interval.

2.2.3. Rotarod test

A rotarod (San Diego Instruments, San Diego, CA) that is capable of rotating at speeds of 4 to 40 rotations per minute (rpm) was used. During the training trials, the rats were trained 3 times at 4 rpm for 60 seconds. Animals that could remain on the rotarod for 60 seconds during the training trials were selected for the test trial. During testing, the rotarod was set to accelerate from 4 to 40 rpm over 300 seconds. The time to fall from the rotarod and the speed at which the rotarod was rotating when the rat fell were recorded. The rotarod tests were performed once per week (1 week prelesion and 5 weeks postlesion).

2.3. RNA extraction, reverse-transcription PCR, and real-time quantitative PCR

Total RNA was extracted using Trizol reagent (Invitrogen, Carlsbad, CA) according to the manufacturer's instructions. Total RNA (2 μg) was used for cDNA synthesis using random hexamers. For the reverse-transcription PCR amplification of BDNF, inducible nitric oxide synthase, vascular cell adhesion molecule 1, tumor necrosis factor α, interleukin 6 (IL-6), IL-10, IL-1β, and interferon γ, initial amplification was performed using each pair of primers, with a denaturation step at 95°C for 10 minutes, followed by 28 cycles of denaturation at 95°C for 1 minute, primer annealing at 55°C for 30 seconds, and primer extension at 72°C for 45 seconds. On completion of the cycling steps, final extension at 72°C for 5 minutes was performed, and then the reaction mixture was stored at 4°C. Real-time quantitative PCR was performed using an ABI PRISM 7500 Sequence Detection System (Applied Biosystems). The reactions were run in triplicate in 3 independent experiments. The geometric mean of the housekeeping gene GAPDH was used as an internal control to normalize variability in expression levels. The expression data were normalized to the geometric mean of the housekeeping gene GAPDH to control variability in expression levels and analyzed using the $2^{-\Delta\Delta CT}$ method described by Livak and Schmittgen.[38] The primer sequences are provided in the Supplementary Table S1 (available online at http://links.lww.com/PAIN/A406).

2.4. Electrophysiological recordings and in vivo microinjection

Electrophysiological recordings were performed 4 weeks after the induction of CPSP. All the electrophysiological data were processed using a multichannel data acquisition system (Tucker-Davis Technologies, Alachua, FL). The sampling rate of the field potential data recording was 6 kHz, and the sampling rate for unit data recording was 24 kHz. Extracellular field potentials were recorded using a multichannel probe (NeuroNexus, Ann Arbor, MI) under maintenance anesthesia with 1.5% isoflurane. For local field potential coherence measurements, an electrode was placed in the right anterior cingulate cortex ([ACC]; 2.5 mm anterior, 1 mm lateral to bregma). For single-unit recordings, an electrode was placed in the MT (2.2-3.5 mm posterior, 0.5-1.0 mm lateral to bregma). The left sciatic nerve was isolated and implanted with a stainless-steel wire electrode to deliver constant-current pulses (pause duration = 0.5 ms, interpause duration = 10 seconds; Model 2100, A-M Systems, Carlsborg, WA) for sciatic nerve stimulation (SNS). The minimal effective pulse current that could elicit hind limb vibration was measured as the 1-fold threshold stimulation strength. Neuronal activity in the

MT was recorded using 1-, 2-, 5-, 10-, and 20-fold increases in the threshold current strength.

2.5. Immunostaining and cell count analysis

After electrophysiological recording, the animals were killed and transcardially perfused with 4% paraformaldehyde in 0.1% phosphate-buffered saline. The brain was collected and post-fixed overnight at 4°C. Brain tissue was incubated with a 30% sucrose/saline solution before cryosectioning (30-40 μm). The cryosections that contained ACC, primary somatosensory cortex (S1), MT, and VB were divided into 3 sets. One set of sections was stained with Cresyl violet, and the other 2 sets were stained with the following primary antibodies: mouse anti-CD11b (1:100, MCA275R, Serotec), mouse anti-NeuN (1:100, MAB377, Millipore), rabbit anti-GFAP (1:200, GTX108711, Genetex), and rabbit anti-P2X4 (1:500, Alomone, APR-002). The secondary antibodies were Alexa Fluor-488 goat anti-mouse IgG (H+L) antibody (1:400, A11001, Life Technologies) and Alexa Fluor-568 goat anti-rabbit IgG (H+L) antibody (1:400, A11011, Life Technologies). DAPI (1 μg/mL, D21490, Life Technologies) was used for nuclear counterstaining.

After immunohistochemistry, 4 sections with visible lesions from the center were chosen for image analysis. Stacks of images at 2 μm increments in depth were collected using a confocal microscope (LSM780, Zeiss), Zen (Zeiss) software, and either a ×20 air objective (NA 0.7) for automatic full section scans or ×40 oil objective (NA 1.3-1.4) for small-field single-cell distinguishable images. The continual disruption of tissue organization and/or loss of staining were identified as the lesion area that should cover the lateral thalamic nucleus. The edges of the lesion were marked in individual sections, and 200 μm distances from the edges of the lesion were chosen as the distant field, the area of which (μm^2) was the region of interest, measured using ImageJ software (National Institutes of Health, Washington, DC) with calibrated parameters from the image acquisition. Supplementary Fig. S1 shows the way in which the region of interest was marked for cell counts (available online at http://links.lww.com/PAIN/A406). Any positive signal less than 5 μm or not accompanied by a DAPI signal was rejected as a false signal. Cells were manually counted within the distant field using ImageJ software.

2.6. Western blot

Tissue was homogenized in lysis buffer that contained 0.1X phosphate-buffered saline, 1% Triton X-100, and complete protease inhibitor cocktail (Roche), pH 7.4. Lysates were clarified by centrifugation at 12,000 rpm for 15 minutes, and the titration of protein concentration was determined using the Pierce BCA protein assay kit (Thermo). The loading amount of each sample was 20 μg. Proteins were separated by 8% sodium dodecyl sulfate-polyacrylamide gel electrophoresis (SDS-PAGE; 7% SDS-PAGE for NKCC1 separation) and then transferred to a polyvinylidene difluoride membrane (Millipore). After blocking with 5% skin milk/TBST for 1 hour at room temperature, the membranes were incubated overnight at 4°C with the following primary antibodies diluted in 0.5% nonfat skin milk/TBST: rabbit anti-KCC2 (1:1000, Millipore), rabbit anti-pKCC2 (Ser940, 1:1000, Rockland), rabbit anti-GABA$_A$ α2 subunit (1:1000, AbCam), rabbit anti-TrkB (1:1000, AbCam), rabbit anti-NKCC1 (1:400, AbCam), and mouse anti-tubulin (1:2500, Sigma). After 3 washes in TBST, the membranes were incubated with species-specific horseradish peroxidase-conjugated secondary antibody

for 45 minutes at room temperature and then revealed using an electrochemiluminescence kit (SuperSignal West Pico kit, Thermo).

2.7. Digital data processing and statistical analysis

Electrophysiology data were transformed and processed using MatLab (MathWorks, Natick, MA). Spontaneous and SNS-induced unit activity was recorded in the MT. The raw data were digitally filtered to determine multiunit spike activity. The coherence coefficient analysis was performed according to the methods of Llinas.[26] Spontaneous local field potentials of deep layer 2/3 or upper layer 5 were transformed using the fast Fourier transform method. For the local field potential data sequence, x_n, an N-sample time series, basic quantity in the wave spectrum estimation at frequency k was discrete Fourier transformed using the following equation:

$$X_k = \sum_{n=0}^{N-1} x_n e^{-i2\pi nk/N}, k = 0, ..., N-1$$

The power spectrum is given by $X_k(t) = |X_k|^2$.

The coherence coefficient, R, between 2 frequency power spectra, $X_A(t)$ and $X_B(t)$, was calculated by the Pearson correlation coefficient method:

$$R = \frac{\sum_t \left(X_A[t] - \overline{X_A}\right)\left(X_B[t] - \overline{X_B}\right)}{\sqrt{\sum_t \left(X_A[t] - \overline{X_A}\right)^2 \sum_t \left(X_B[t] - \overline{X_B}\right)^2}}$$

where $\overline{X_A}$ and $\overline{X_B}$ are the mean values of $X_A(t)$ and $X_B(t)$, respectively.

Each coherence coefficient was calculated based on 10 to 15 minutes of continuous spontaneous oscillation local field potential data, with a moving time window of 10 seconds. By loop calculating the coherence coefficient between 1 to 50 Hz power spectrum, a 2-dimensional correlation image of 1 to 50 Hz spectrum was generated.

All the data were statistically analyzed using unpaired Student t tests, one-way analysis of variance (ANOVA), and two-way ANOVA using SPSS software (Chicago, IL). Values of $P < 0.05$ were considered statistically significant.

3. Results

3.1. Mechanical and thermal allodynia after ventrobasal lesions

The lateral thalamus was lysed by injecting collagenase in the VB. Four weeks after the thalamic lesion, tissue loss and some hemorrhagic sites could be observed around the lesion area (**Fig. 1A**). The lesion area for each animal was primarily located in the VB, with the involvement of nuclei that surrounded the VB (**Fig. 1B**). One week after the lesion, mechanical thresholds in the left hind limb significantly decreased, and thermal allodynia occurred 3 weeks later (**Fig. 1C, D**). The experimental animals developed mechanical and thermal allodynia in the left hind limb 1 to 3 weeks after the hemorrhagic lesion, which persisted for at least 4 weeks compared with the sham control group (von Fret test: mixed 2-way ANOVA, $F_{4,56} = 9.76$, $P < 0.05$; plantar test: mixed 2-way ANOVA, $F_{4,72} = 4.62$, $P < 0.05$). The rotarod test was repeated once per week, and no differences were found between the sham control group (n = 11) and CPSP group (n = 11) during the entire duration of CPSP induction (mixed 2-way ANOVA, $F_{1,21} = 2.58$, $P > 0.05$; Supplementary Fig. S2, available online at http://links.
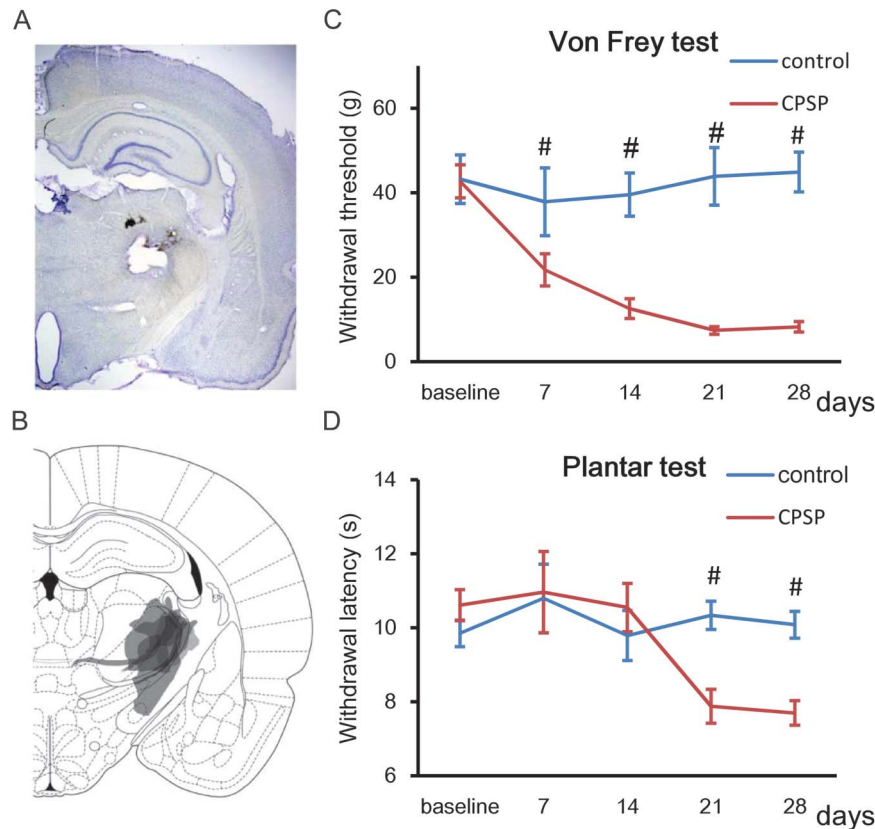
Figure 1. Mechanical and thermal allodynia occurred after ventrobasal (VB) lesions. Before surgery, baseline bilateral hind limb mechanical and thermal thresholds were tested in the von Frey test and plantar test. After collagenase injections in the VB, mechanical and thermal thresholds were recorded on days 1, 3, 7, 14, 21, and 28. (A) Example of collagenase lesion. After the animals were killed, the brains were removed, sectioned at 60 μm, and Nissl-stained. (B) The collagenase lesion areas for each animal were pooled. The shapes of the lesion areas were diverse but surrounded the VB area. (C, D) The von Frey test and plantar test were conducted on the bilateral hind limbs in central poststroke pain animals for 28 days. Mechanical and thermal thresholds decreased after the collagenase lesion, especially 14 days after lesion. Although the data that are presented in the figure end on day 28, we found that the decrease in thresholds was maintained for more than 40 days. #$P < 0.05$ (2-way analysis of variance followed by post hoc test). Control group, n = 8. Central poststroke pain group, n = 8.

lww.com/PAIN/A406). These results indicate that the sham and VB lesion groups did not exhibit differences in motor performance in the rotarod task.

3.2. Proliferation of astrocytes and microglia 30 days after thalamic lesion

Wasserman reported that thalamic lesions alter the cellular composition. After the induction of CPSP, neuronal loss and astrocyte and microglial proliferation or infiltrated macrophages were found 1 to 7 days after the thalamic lesion.[36] Because the currently available antibodies could not well distinguish the microglia and posttraumatic infiltrated macrophage, later description in our study will use the term to note the results originally from the immunolabeling of microglia as microglia/macrophage. Similar results were found 4 weeks after the thalamic lesion. Neuronal loss (indicated by NeuN staining), astrocyte proliferation (indicated by GFAP staining), and microglial (indicated by CD11b staining) proliferation or infiltrated macrophages occurred 1 month after the thalamic lesion (**Fig. 2A**). The cell density of neurons, astrocyte, and microglia/macrophage (number/mm²) on the lesion side (ie, right side of the MT) and contralateral side was counted (**Fig. 2B**). To determine the relationship between the development of allodynia and changes in the cellular composition after CPSP, we examined the ratio of mechanical threshold ([RM] =

withdraw strength on day 28/withdraw strength on day 0; left hind limb) and the ratio of cell density changes ([RCD] = cell density of the perilesion area/cell density of the same area on the left side) after CPSP. The linear regression analysis of the RM and RCD was conducted ($Y = 0.345X + 49.522$, $R^2 = 0.525$, $P < 0.05$, Supplementary Fig. S3, available online at http://links. lww.com/PAIN/A406). These results indicate that if fewer neurons survive after the lesion, the degree of allodynia would be more serious. Linear regression analyses of the RM and RCD of glia and microglia/macrophage were also conducted (glia: $Y = -0.206X + 156.41$, $R^2 = 0.532$, $P < 0.05$; microglia: $Y = -0.14X + 138.695$, $R^2 = 0.565$, $P < 0.05$). This indicates that the greater proliferation of glia or microglia/macrophage in the perilesion area after the lesion resulted in greater allodynia. Tissue samples from the perilesion sites were analyzed by quantitative real-time quantitative PCR. The expression of BDNF and other inflammatory factors (ie, tumor necrosis factor α, IL-6, IL-10, IL-1b, and IFNγ) significantly increased in perilesion tissues compared with the contralateral unaffected sites (**Fig. 2C**). A link between BDNF and P2X4 receptor activation has been reported.[34] The synthesis and secretion of BDNF by microglia/macrophage are activated by high concentrations of adenosine triphosphate that leaks from injured tissue. Our data indicate that both microglia/macrophage and P2X4 receptors were activated in perilesion tissue (**Fig. 2A**), which may be a source of BDNF overexpression. The results
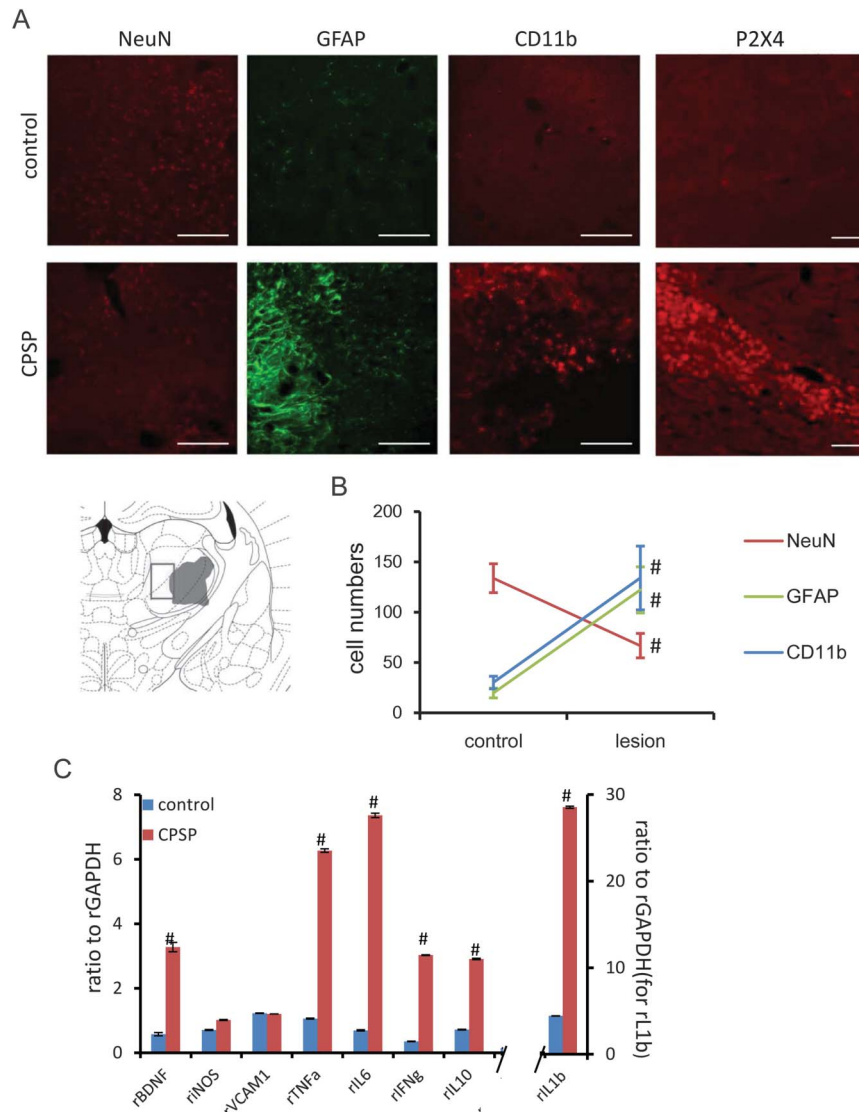
Figure 2. Astrocyte and microglial cell scars were still evident 30 days after the collagenase lesion. After the animals were killed, 30-μm brain slices were prepared for immunostaining. (A) Immunostaining with NeuN (neurons), GFAP (astrocytes), and CD11b (microglia) and P2X4 receptor expression in the perilesion area. Scale bar = 200 μm. (B) Cell number in 500 μm² perilesion area (right brain, Les) and unlesioned area (left brain, Con). In the ventrobasal perilesion area, neuronal loss was significantly higher than in the left-side brain area. The figure shows high glial and microglial proliferation in the lesion area. (C) Tissue samples from the perilesion sites were analyzed by quantitative real-time quantitative PCR. The expression of brain-derived neurotrophic factor and inflammatory cytokines was assessed. #$P < 0.05$ (paired t test). Control and central poststroke pain groups, n = 10.

confirmed our previous findings,[23] indicating that the activity of tissue repair mechanisms and inflammation was still very strong in the perilesion area.

3.3. Enhancement of the noxious response in the medial thalamus was widespread in central poststroke pain animals

Abnormal thalamic neuronal hyperactivity is an important characteristic of CPSP. The power density of single-photon emission computed tomography images in the thalamus was previously shown to be enhanced in some CPSP patients.[3] The MT is an important relay site in the medial pain processing pathway. We recently observed enhanced neuronal hypersensitivity in the MT in CPSP.[23] In this study, the rats were maintained under light isoflurane anesthesia and implanted with a multichannel electrode in the MT, and a noxious electric shock was applied to the sciatic nerve (**Fig. 3A**). Neuronal activity of the MT was

evoked by noxious SNS (**Fig. 3B**). The noxious response of the MT was evoked after 100 to 150 ms of stimulation. The duration and amplitude of evoked activity were stable after repeated stimulation. In CPSP animals, an enhanced and prolonged noxious response was evoked by repeated noxious stimulation (**Fig. 3C**). This prolonged noxious neuronal activity was maintained for >1 second. The summation of multiunit activity was 0 to 1500 milliseconds after stimulation (20 sweeps). A wind-up effect was found in CPSP animals after 3 trains of electrical stimulation (**Fig. 3D**). Multistrength electric shock responses were also measured. The ratio between stimulation strength and MT neuronal activity after wind-up is shown in **Figure 3E**. The duration of the normal evoked noxious responses was within the 80 to 150 milliseconds time window after electrical stimulation. The evoked noxious response could be separated into a fast component (within 200 ms after stimulation, 20 sweeps) and late component (200-2000 ms after stimulation, 20 sweeps). The
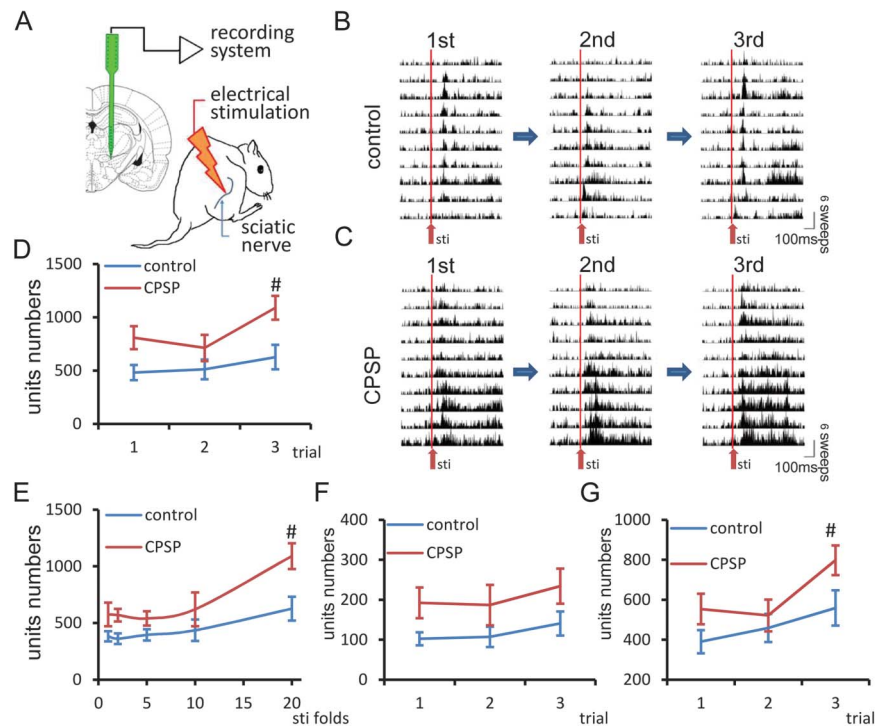
Figure 3. Enhancement of the noxious response in the medial thalamus (MT) was widespread in central poststroke pain (CPSP) animals. A neuronal wind-up noxious response was observed in the MT in CPSP animals. To record the noxious response in the MT area, neuronal multiunit activity was recorded using a multichannel electrode accompanied by sciatic nerve stimulation. (A) Orientation of multichannel probe and sciatic nerve stimulation (SNS). (B) Multiunit responses in the MT after repeated noxious electrical stimulation of the sciatic nerve were not significantly changed in control rats. (C) In CPSP animals, repeated electrical stimulation enhanced the noxious response of the MT, which extended to more than 1 second. (D) Summation of multiunit responses within 2000 ms after sciatic nerve stimulation over 3 trials. (E) To compare the noxious response of the MT between groups, different stimulation strengths were applied. The number of multiunit responses after low-strength electrical stimulation was similar between groups. After high-strength electrical stimulation, the noxious response of the MT was significantly higher in the CPSP group than in the control group. (F, G) Summation of multiunit responses of the fast component (within 0-200 ms after SNS) and late component (within 200-2000 ms after SNS) over 3 trials.

wind-up effect occurred in the late component but not in the fast component (**Fig. 3E**).

3.4. Enhancement of nociceptive response in the medial thalamus was suppressed by TrkB-Fc

Brain-derived neurotrophic factor is an important neuronal trophic factor that is secreted by astrocyte/glial cells or microglia/macrophages and has been suggested to be involved in neuropathic pain. The proliferation of astrocyte/glial cells and increase in P2X4 receptor expression suggest the involvement of a separate mechanism of CPSP through BDNF. Right-side MT tissues in CPSP rats and nonlesion control rats were analyzed by Western blot (**Fig. 4A**). The BDNF expression in the CPSP group was higher than in the control group. The average level of expression of TrkB receptors was not influenced by the thalamic lesion (**Fig. 4A**). To examine the influence of BDNF in CPSP animals, nociceptive tests were performed in freely moving rats. Seven days after recovering from cannula implantation in the upper side of the MT, control rats were microinjected with TrkB-Fc (1.0 μg/μL/d), and CPSP rats were microinjected with dTrkB-Fc (1.0 μg/μL/d), TrkB-Fc (1.0 μg/μL/d), or CTX-B (0.5 μL of solution, 10 μg/μL/d) through the cannula. One to 1.5 hours after the injection, the von Frey and plantar tests were performed.

In the von Frey test, thresholds in the control-TrkB-Fc, CPSP-dTrkB-Fc, CPSP-TrkB-Fc, and CPSP-CTX-B groups were significantly different (4×6 mixed 2-way ANOVA, $F_{3,22} = 29.45.97$, $P <$

0.05), with a significant effect of days ($F_{5,110} = 8.23$, $P < 0.05$) and a significant group $\times$ days interaction ($F_{15, 110} = 3.94$, $P < 0.05$; **Fig. 4B**). The Tukey post hoc test indicated that mechanical thresholds in control animals were not influenced by the TrkB-Fc injection from day 37 to day 40 ($P > 0.05$; **Fig. 4B**). Mechanical thresholds gradually increased after the TrkB-Fc or CTX-B injection in CPSP animals compared with the control-TrkB-Fc and CPSP-TrkB-Fc/CPSP-CTX-B groups ($P > 0.05$; from day 37 to day 40 but not for day 35 or 36). Therefore, the BDNF scavenger and TrkB receptor antagonist significantly reduced the effect of CPSP (**Fig. 4B**). The CPSP-dTrkB-Fc group exhibited mechanical allodynia compared with the control-TrkB-Fc group ($P < 0.05$). In the plantar test, thermal allodynia in CPSP animals was not significantly reduced by TrkB-Fc or CTX-B treatment (Supplementary Fig. S4, available online at http://links.lww.com/PAIN/A406).

To confirm the influence of BDNF after CPSP, the BDNF scavenger TrkB-Fc was infused into the MT (1 μg/μL/4 min) in CPSP animals (**Fig. 4C**). The evoked response in the MT was not significantly altered by dTrkB-Fc in CPSP rats (**Fig. 4D, F**). One to 2 hours after the acute infusion of TrkB-Fc, the enhanced MT-evoked response decreased and then recovered after 4 hours (**Fig. 4E, G**). Both the fast component (within 200 ms after stimulation; $P < 0.05$; **Fig. 4H**) and late component (200-2000 ms after stimulation; $P < 0.05$; **Fig. 4I**) significantly decreased after the TrkB-Fc injection (fast component, mixed 2-way ANOVA, $F_{1,10} = 6.69$, $P < 0.05$, at 60, 120, and 180 minutes; late component, mixed two-way ANOVA, $F_{1,10} = 4.62$, $P < 0.05$, at 60 and 120 minutes).
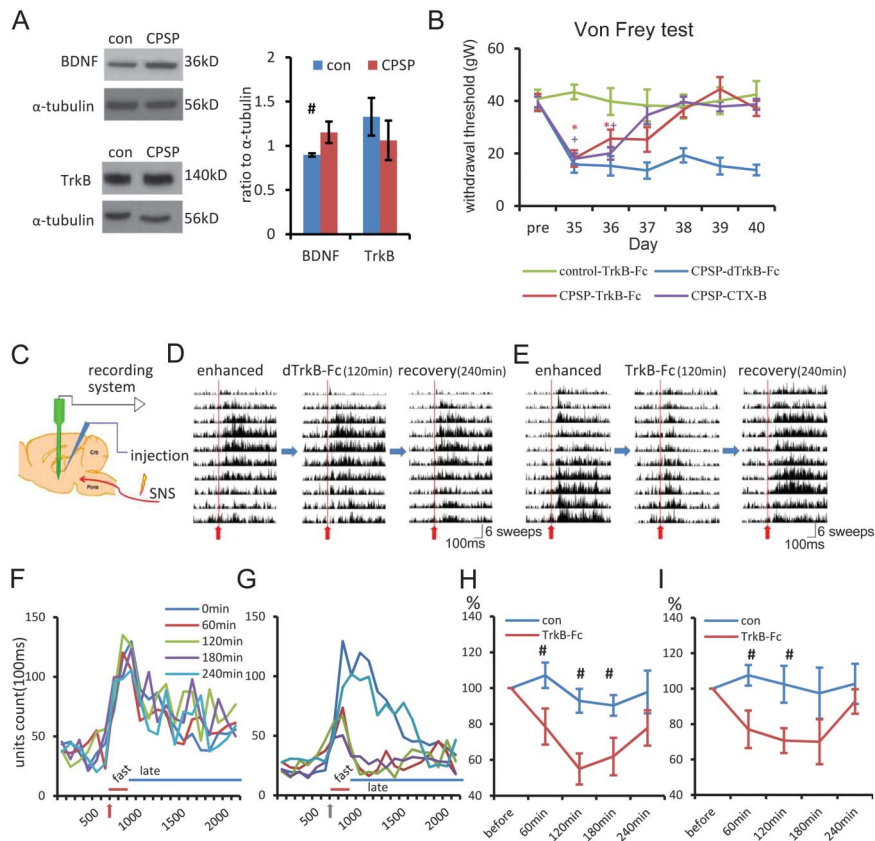
Figure 4. Mechanical allodynia and enhancement of the noxious response in the medial thalamus (MT) were suppressed by TrkB-Fc application. (A) The BNDF and TrkB receptor expression in the MT in the central poststroke pain (CPSP) group, analyzed by Western blot. #$P < 0.05$ (t test). (B) Changes in mechanical thresholds after microinjections of dTrkB-Fc, TrkB-Fc, and CTX-B in CPSP animals. #$P < 0.05$, control-TrkB-Fc group compared with CPSP-TrkB-Fc group or CPSP-CTX-B group (mixed 2-way analysis of variance [ANOVA], followed by post hoc test). #$P < 0.05$, control-TrkB-Fc group compared with CPSP-dTrkB-Fc group (mixed 2-way ANOVA, followed by post hoc test). (C) Orientation of multichannel probe and acute microinjection. (D, E) To examine the influence of the brain-derived neurotrophic factor, the brain-derived neurotrophic factor scavenger TrkB-Fc was injected in the MT, and noxious responses were recorded in CPSP animals. The wind-up noxious response was not influenced by dTrkB-Fc. One to 2 hours after the TrkB-Fc injection, however, the enhanced noxious response of the MT decreased and recovered after 180 to 240 minutes. (F, G) Time series plot of summation of multiunit responses (100 ms bins; red arrow indicates sciatic nerve stimulation) before and after the dTrkB-Fc (F) or TrkB-Fc (G) microinjection. (H, I) Time series plot of fast component (H) and late component (I) of MT activity induced by sciatic nerve stimulation before and after the dTrkB-Fc or TrkB-Fc microinjection. #$P < 0.05$ (2-way ANOVA, followed by post hoc test).

3.5. Spontaneous medial thalamus activity was enhanced by a GABA$_A$ receptor agonist in central poststroke pain rats

The involvement of GABAergic mechanisms in BDNF over-expression has been previously revealed in studies of neuropathic pain and spinal cord injury. The expression of the cotransporter KCC2 and GABA$_A$ receptors in right-side MT tissue in CPSP animals was significantly lower than in control animals (**Fig. 5A, B**). The expression of phospho KCC2 in the CPSP group was higher than in the control group (**Fig. 5A, B**). The expression of the cotransporter NKCC1 was not significantly different between groups (**Fig. 5A, B**). The significant increase in pKCC2 and decreases in KCC2 and GABA$_A$ receptors in CPSP animals may influence the accumulation of [Cl$^-$]$_{in}$. Alterations of spontaneous thalamic unit activity that was induced by the GABA$_A$ receptor agonist muscimol were tested. Spontaneous multiunit activity was recorded and analyzed using multichannel electrodes in the MT. Spontaneous multiunit activity was silenced 10 to 20 minutes after muscimol perfusion (50 μM/0.1 μL/4 min) in the MT, which recovered 2 hours later in the sham control group (**Fig. 5C, E**, left panel). By contrast, the average firing rate of spontaneous multiunit activity was higher in the CPSP group and greatly enhanced by muscimol treatment (**Fig. 5D, E**, right panel). Muscimol-induced enhancement was maintained for 20 to 30 minutes (two-way ANOVA followed by post hoc test, $P < 0.05$; **Fig. 5F**) and gradually recovered 1 hour later. These results indicate that the inhibitory function of the GABA system was altered after the development of CPSP. To evaluate alterations of the expression of the cotransporter KCC2 in CPSP, KCC2 expression was examined in the right MT after CPSP induction with and without TrkB-Fc treatment. After repeated injections of TrkB-Fc, the expression of KCC2 in the CPSP-TrkB-Fc group significantly increased compared with the CPSP group (**Fig. 6A**). These results indicate that KCC2 downregulation in the CPSP group was reversed by TrkB-FC treatment. The expression of oligomers of KCC2 in the MT was not significantly different between the sham control group and CPSP group (t test, $P > 0.05$, n = 5; **Fig. 6B**). Therefore, the specific effect of TrkB-FC treatment on these oligomers was not tested.

3.6. Coherence coefficients of local field potentials were enhanced in central poststroke pain rats

Coherence coefficients of spontaneous magnetoencephalo-graphic oscillations have been shown to be enhanced in Parkinson disease, tinnitus, neurogenic pain, and major de-pression, which may be induced by thalamocortical dysrhythmia
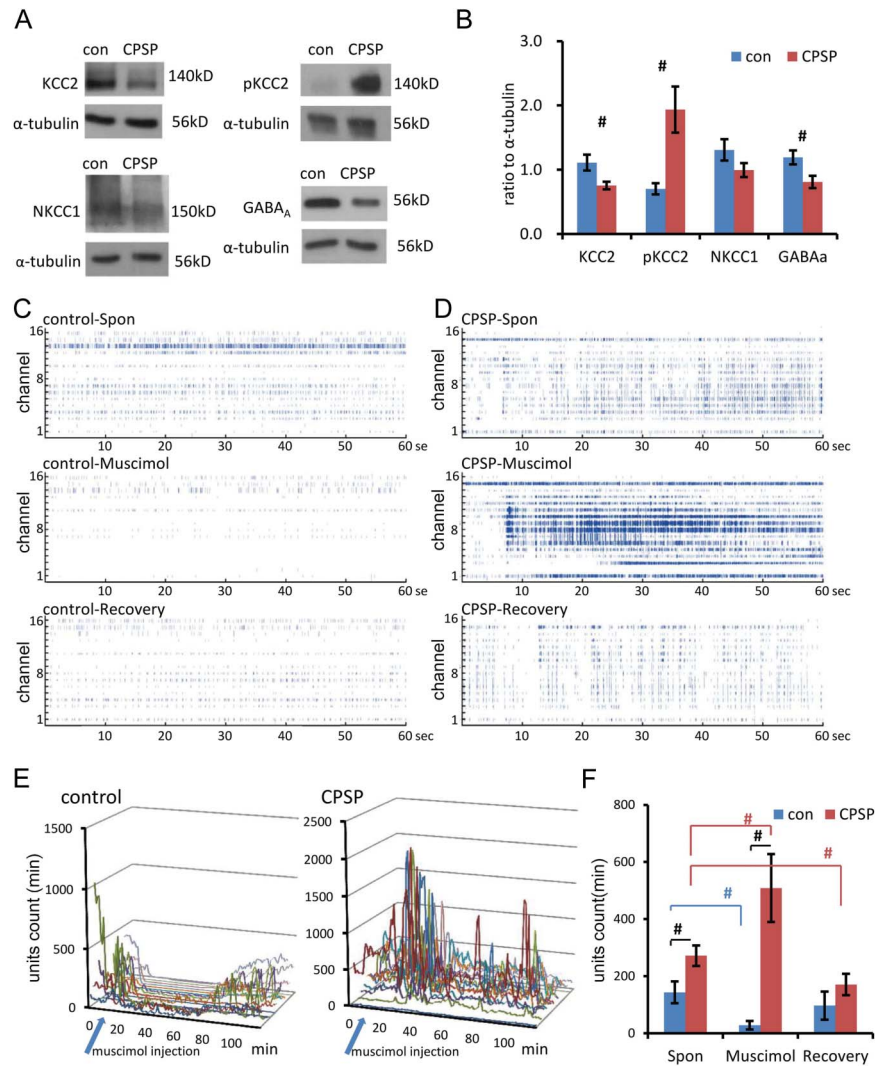
Figure 5. Spontaneous medial thalamus (MT) activity was enhanced by a GABA$_A$ receptor agonist. (A, B) Expression of the cotransporter KCC2, phospho KCC2 (Ser940), cotransporter NKCC1, and GABA$_A$ receptors, analyzed by Western blot. (C, D) Summation of MT spontaneous multiunit activity recorded by a multichannel electrode. An example from a control animal is shown in C, and an example from a central poststroke pain (CPSP) animal is shown in D. After the muscimol injection in the MT, control multiunit activity decreased, but CPSP multiunit activity increased. The effect of muscimol was maintained for 2 to 3 hours. (E) Time plot of spontaneous multiunit responses before and after the muscimol injection. (F) Average MT unit activity in the control and CPSP groups before and after the muscimol injection. Spontaneous activity in the CPSP group was higher than in the control group. In control animals, enhanced GABA activity inhibited neuronal activity in the MT. In CPSP animals, the inhibitory GABA system appeared to be reversed, and muscimol treatment enhanced neuronal activity in the MT. #$P < 0.05$ (2-way analysis of variance followed by post hoc test). Control group, n = 6. CPSP group, n = 8.

oscillations.[26] In our previous study, the ACC-MT thalamocortical pathway was shown to transmit noxious information. After CPSP induction, the spontaneous activity and sensitivity of MT neurons were altered. An interesting issue is whether the neuronal oscillation pattern in the ACC is influenced by abnormal neuronal oscillations in the MT after CPSP. Greater coherence coefficients of spontaneous local field potentials were found in the ACC in CPSP animals (**Fig. 7A, B**). The enhanced coherence coefficients
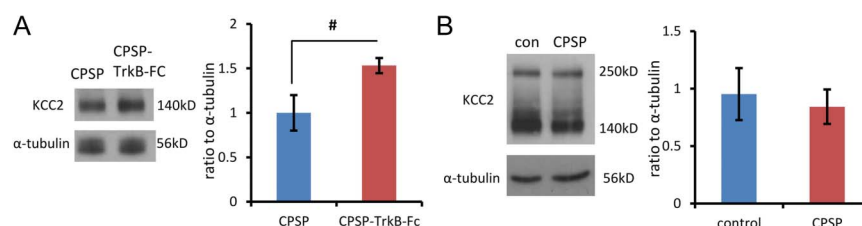

Figure 6. The effect of TrkB-Fc treatment on the expression of KCC2. (A) The expression of KCC2 was measured in the medial thalamus in central poststroke pain animals that were or were not treated with TrkB-Fc. The expression of KCC2 significantly increased after TrkB-Fc treatment. (B) The expression of KCC2 oligomers (~250kD) was not significantly different between the central poststroke pain group (n = 5) and sham control group (n = 5).
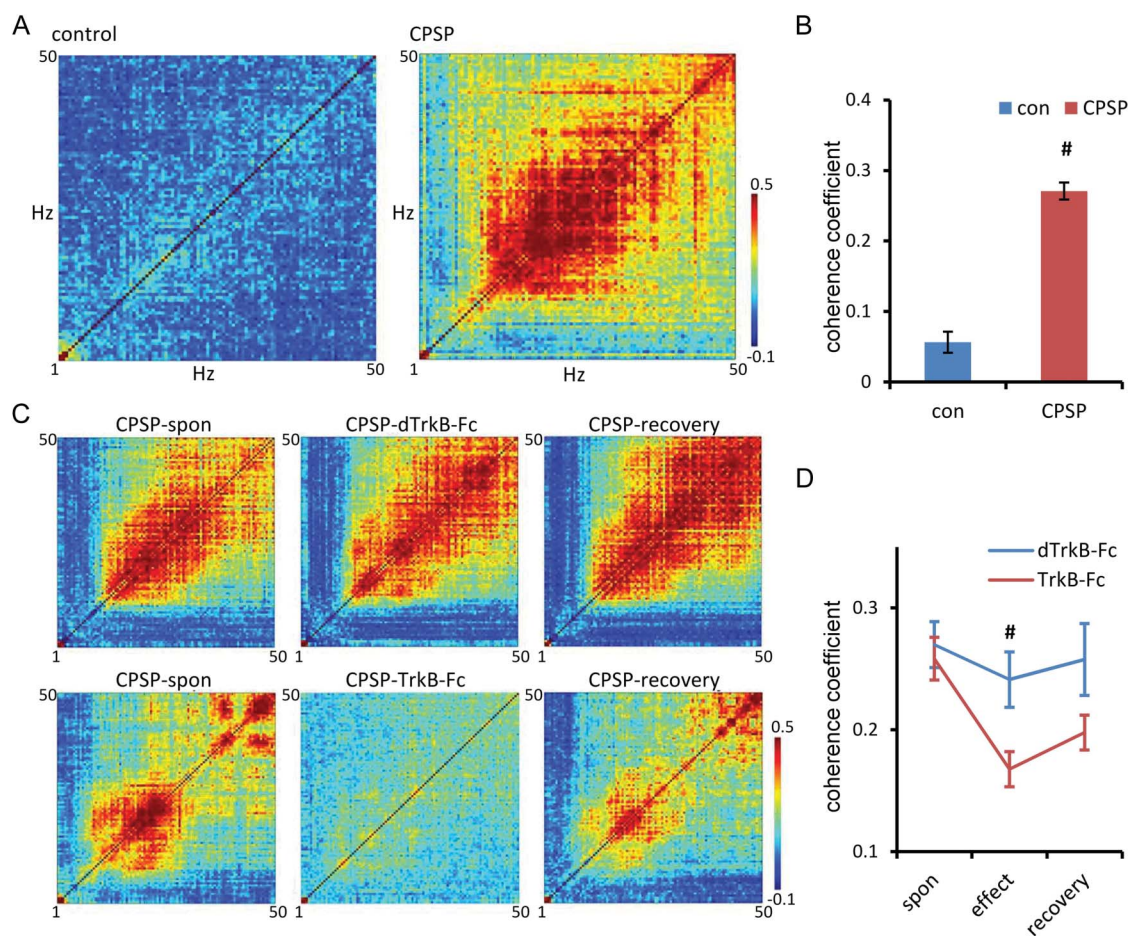
Figure 7. Coherence coefficients of local field potentials were enhanced in central poststroke pain (CPSP) rats. (A) Coherence coefficient patterns of spontaneous local field potentials between 1 and 50 HZ in the anterior cingulate cortex in the control and CPSP groups. (B) Average coherence coefficients between 10 and 50 Hz in the control and CPSP groups. (C) Patterns of coherence coefficients of spontaneous local field potentials between 1 and 50 HZ in the anterior cingulate cortex in CPSP animals that received microinjections of dTrkB-Fc or TrkB-Fc in the medial thalamus. (D) Average coherence coefficients between 10 and 50 Hz in CPSP animals that received microinjections of dTrkB-Fc or TrkB-Fc.

were observed between the 10 and 50 Hz bands. The patterns of enhanced coherence coefficients were similar between magnetoencephalographic oscillations in CPSP patients and local field potentials in CPSP animals. The enhanced coherence coefficients could be suppressed by TrkB-Fc. One to 2 hours after the TrkB-Fc microinjection (1 μg/μL) in the VB, the enhanced coherence coefficients were temporarily suppressed (**Fig. 7C**, lower panel, and **Fig. 7D**). This suppression did not occur with dTrkB-Fc treatment (**Fig. 7C**, upper panel, and **Fig. 7D**). These data indicate that cortical dysrhythmia oscillations were induced by thalamic damage, and the suppression of BDNF overexpression may be an effective way to reverse CPSP.

4. Discussion

In this study, mechanical and thermal allodynia was induced by intracerebral hemorrhage (ICH). The proliferation of astrocyte and microglia plus infiltrated macrophages with greater P2X4 receptor expression was found in the perilesion area after ICH. The BDNF and inflammatory factor overexpression was evaluated. The blockade of BDNF cascades by TrkB-Fc and Tat Cyclotraxin-B coaltered central pain conditions. Our data indicate that the noxious response in the MT and oscillation pattern of the thalamocortical pathway were altered in CPSP rats. The neuronal nociceptive responses, oscillation pattern of the thalamocortical

pathway, and allodynia behavior in CPSP rats were reversed to a normal state by TrkB-Fc treatment. Thalamic neurons were found to be excited by the GABA$_A$ receptor agonist muscimol in CPSP rats, which may be attributable to a decrease in expression of the cotransporter KCC2 or enhancement of pKCC2. However, because of the limited number of antibodies we used in this study, it is unknown whether other KCC2 phosphorylation sites may be involved in the pathogenesis of CPSP; it requires further investigation. **Figure 8** shows a schematic drawing based on our findings, illustrating circuit damage that is caused by ICH and changes in molecules/membrane channels after CPSP.

Lesions of the spinal cord are associated with neurochemical, excitotoxic, anatomical, and inflammatory changes, all of which can influence neuronal plasticity and increase neuronal excitability after spinal cord nerve injury.[38] Intracerebral hemorrhage in the thalamus also caused similar anatomical and inflammatory changes, tissue loss, and astrocyte and microglial proliferation. Activated microglial cells secrete BDNF and several other cytokines. Our data indicate that cytokines and BDNF were overexpressed in the thalamus after ICH. The suppression of cytokines and BDNF can relieve allodynia or hyperalgesia after spinal cord nerve injury.[7] Thus, BDNF overexpression in the tissue that undergoes traumatic injury is an important factor in neuropathic pain.[20] The relationship between BDNF and P2X4 receptors has been demonstrated.[34] P2X4 receptor activation
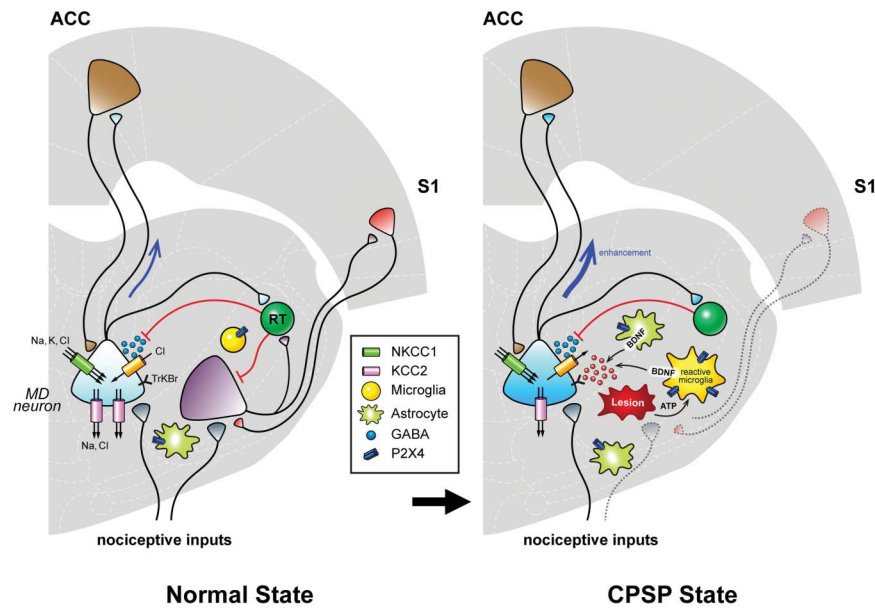
Figure 8. Schematic illustration of the involvement of brain-derived neurotrophic factor (BDNF) in sequential signaling effects on neuronal activity in central poststroke pain. In the normal physiological state, nociceptive inputs are received from peripheral primary afferents to the medial and lateral thalamus. Excitatory MD neurons then pass the ascending input to the anterior cingulate cortex and S1 to generate pain perception. The reticular thalamic nucleus neurons synergistically project inhibitory synapses to provide controls through known GABAergic inhibitory machinery, including NKCC1 and KCC2. Resident microglia and astrocytes remain in their basal condition, and normal levels of BDNF do not alter the ionic flow that passes through KCC2 and GABA receptors through TrkB receptor modulation. In the pathological state, such as central poststroke pain, these traumatized cells at the lateral thalamic lesion site release a high amount of intracellular molecules, triggering the activation of microglia and proliferation of astrocytes in the surrounding tissues. Along the lesion site, wounded cells release ATP, which results in the activation of P2X4 receptors and higher levels of BDNF that overbind TrkB receptors, thus inducing downstream inhibition of KCC2, reversing the flow of chloride ions through GABA receptors, and contributing to the disinhibition of lateral thalamic inhibitory inputs to the medial thalamus. This results in the enhancement of neuron bursting activity along the thalamocingulates pathway.

causes the phosphorylation of p38-mitogen–activated protein kinase, resulting in the release of BDNF. The intracellular signaling by which P2X4 receptor stimulation drives the synthesis and release of BDNF is essential to the persistence of pain hypersensitivity after nerve injury.[34] A recent study found that morphine-induced hyperalgesia that occurred through the P2X4R-BDNF-KCC2 disinhibition cascade between microglia and spinal dorsal horn neurons interfered with principal nodes in the cascade to suppress hyperalgesia.[10] Clarifying the interaction between P2X4 and P2X7 receptors and their downstream targets may help elucidate the mechanism of microglial activation and proliferation after neural trauma and provide insights into the development of CPSP treatment.

The ICH model has been widely used in stroke research. Hemorrhagic sites and tissue damage can be found in the brain a few days after collagenase injection. Intracerebral hemorrhage did not affect performance in the rotarod test.[15] Our study revealed no significant difference in the rotarod test, indicating that allodynia that is induced by ICH is not attributable to motor deficits of the hind limb.

Thalamic hyperactivity has been observed in CPSP patients using single-photon emission computed tomography.[5,29] We found that both spontaneous neuronal activity and the noxious response of the MT were enhanced after the development of CPSP. Another possibility is a decrease in a feedforward or feedback inhibition mechanism in the thalamocortical pathway after CPSP. Our study revealed that spontaneous neuronal activity in the MT was enhanced after muscimol application in CPSP animals. This indicates a deficient inhibitory mechanism of the thalamocortical pathway after CPSP, and abnormal enhanced reverberation was induced in the spontaneous

oscillations or in the nociceptive response that caused neuropathic pain after hemorrhagic stroke.

Brain-derived neurotrophic factor is an important modulator of neuronal plasticity. Serum BDNF concentrations have been correlated with mechanical and thermal pain thresholds in healthy female subjects.[33] The BDNF overexpression in pathological tissue was positively correlated with chronic pain processing in chronic pancreatitis patients.[41] In rodent models, neuropathological pain developed a few days after spinal cord nerve injury. The BDNF overexpression was found in injured tissue and dorsal root ganglia. After repeated intrathecal injections of TrkB-Fc, mechanical allodynia was gradually reduced. Recent studies indicate that BDNF expression is induced by microglial cell proliferation.[8,12,40] We also found that BNDF expression in the thalamus in the CPSP group was higher than in the control group. Three days after the TrkB-Fc microinjection in the lesion area, mechanical allodynia was reduced. This indicates that the suppression of BNDF overexpression may be an effective treatment for CPSP.

The neuronal plasticity of MT neurons and thalamocortical oscillation patterns were altered after CPSP induction. Abnormal neuronal activity and oscillation patterns could be temporarily reversed by microinjections of TrkB-Fc immediately after CPSP induction. Mechanical allodynia was also reduced by daily repeated microinjections of TrkB-Fc. Protein synthesis is influenced by the acute application of BDNF.[18] We propose that the acute effect of TrkB-Fc may influence protein synthesis and reverse the decreased KCC2 level in CPSP. However, we cannot exclude the possibility that acute TrkB-Fc application modulates neuronal plasticity. Synaptic transmission and long-term potentiation were previously shown to be induced within 1 hour after

BDNF application in mature hippocampal neurons.[11,18,21] Neuronal activity and the long-term potentiation of mature hippocampal neurons were decreased by TrkB-IgG application.[11] In our study, we found that the nociceptive activity of MT neurons increased and nociceptive thresholds of mechanical and thermal stimulation decreased after CPSP induction. The increases in neuronal activity in the MT were reduced by acute TrkB-Fc application, and the relief of mechanical allodynia occurred in CPSP animals after daily repeated TrkB-Fc micro-injections in the MT. These effects may influence thalamocortical oscillations, reflected by the mitigation of abnormal thalamocortical oscillations after TrkB-Fc treatment. Our data suggest that BDNF is an important factor that modulates central pain. Intrathecal BDNF application was shown to induce mechanical and thermal allodynia in rodents.[4,14,37] In a spinal cord nerve injury model, an increase in BDNF expression was shown to be an important factor in mechanical and thermal allodynia. Mechanical or thermal allodynia that is induced by nerve injury or inflammation was shown to be relieved by TrkB-Fc treatment.[4,37]

$[Cl^-]_{in}$ in neurons is controlled by the cotransporters KCC2 and NKCC1. In neonatal neurons, NKCC1 is abundant, and $[Cl^-]_{in}$ is higher than $[Cl^-]_{out}$. After neurons mature, KCC2 dominates the balance of $[Cl^-]$, in which $[Cl^-]_{in}$ is lower than $[Cl^-]_{out}$. The ratio of the composition of KCC2 and NKCC1 is controlled by the level of BDNF expression. The expression of NKCC1 is enhanced by BDNF, and KCC2 expression is decreased by BDNF. After ICH, the expression of BDNF in the thalamus is higher than normal, and the ratio of the composition of KCC2 and NKCC1 changes to an immature state, which may cause $[Cl^-]_{in}$ to be lower than $[Cl^-]_{out}$. Because of the accumulation of $[Cl^-]_{in}$, the inhibitory effect of GABA switches to an excitatory effect after CPSP. The balance of thalamocortical circuits is controlled by either feedforward or feedback inhibition. Based on the present results, we hypothesize that the inhibition circuit from the reticular thalamic (RT) nucleus to thalamic relay neurons switches to an excitation circuit after CPSP, which is caused by $[Cl^-]_{in}$ accumulation in relay neurons. According to the retrograde tracing results in the medial dorsal thalamic nucleus,[13] projections from the RT to medial dorsal thalamic nucleus mainly originate from the anterior part of the RT. In this study, the lesion area included most of the caudal RT, and the anterior part of the RT was well preserved. Thus, we assume that most of the RT and MT connections remained intact. Additional mechanisms of excitation in damaged sensory pathways and the effects of impaired inhibitory pathways have been suggested.[2,3,6,16,35] One such hypothesis involves the disinhibition theory, which was first proposed by Holmes.[16] This theory suggests that injury to the lateral thalamus frees the MT from its control. Additionally, the thermosensory disinhibition theory suggests that CPSP results from impairment of the normal inhibition of pain from cold signals owing to a lesion. Such damage produces an imbalance between a pathway that is involved in signaling cold sensations and a medial pain pathway.[6] An alternative theory of the disinhibition of medially located spinoreticulothalamic or paleospinothalamic pathway by lesions of the lateral spinothalamic tract has also been proposed.[3] Recent animal studies provided evidence that central pain results from maladaptive homeostatic plasticity that is caused by the loss of normal ascending inputs through spinothalamic tracts.[35] Moreover, dynamic reverberation theory suggests that central pain results from alterations of processing inside a corticothalamocortical reverberatory loop and extends throughout widespread areas of the brain.[2] The present results support an imbalance between the lateral and MT, and

abnormal excitability in the MT resulted as disinhibition from the injury of lateral thalamus through the reversal of the GABA function in the RT in the CPSP condition. Future studies should evaluate chloride homeostasis in MT neurons and transformation of the modulatory effects of the reticular thalamic nucleus after CPSP.

Conflict of interest statement

The authors have no conflicts of interest to declare.

Acknowledgements

Appendix A. Supplemental Digital Content

Supplemental Digital Content associated with this article can be found online at http://links.lww.com/PAIN/A406.

References

[1] Bowsher D. Stroke and central poststroke pain in an elderly population. J Pain 2001;2:258–61.

[2] Canavero S. Dynamic reverberation—a unified mechanism for central and phantom pain. Med Hypotheses 1994;42:203–7.

[3] Cesaro P, Mann MW, Moretti JL, Defer G, Roualdes B, Nguyen JP, Degos JD. Central pain and thalamic hyperactivity—a single photon-emission computerized tomographic study. PAIN 1991;47:329–36.

[4] Coull JAM, Beggs S, Boudreau D, Boivin D, Tsuda M, Inoue K, Gravel C, Salter MW, De Koninck Y. BDNF from microglia causes the shift in neuronal anion gradient underlying neuropathic pain. Nature 2005;438:1017–21.

[5] Coull JAM, Boudreau D, Bachand K, Prescott SA, Nault F, Sik A, De Koninck P, De Koninck Y. Trans-synaptic shift in anion gradient in spinal lamina I neurons as a mechanism of neuropathic pain. Nature 2003;424:938–42.

[6] Craig ADB. A new version of the thalamic disinhibition hypothesis of central pain. Pain Forum 1998;7:1–14.

[7] Deng YS, Zhong JH, Zhou XF. Effects of endogenous neurotrophins on sympathetic sprouting in the dorsal root ganglia and allodynia following spinal nerve injury. Exp Neurol 2000;164:344–50.

[8] Elkabes S, DiCiccoBloom EM, Black IB. Brain microglia macrophages express neurotrophins that selectively regulate microglial proliferation and function. J Neurosci 1996;16:2508–21.

[9] Feigin VL, Lawes CM, Bennett DA, Anderson CS. Stroke epidemiology: a review of population-based studies of incidence, prevalence, and case-fatality in the late 20th century. Lancet Neurol 2003;2:43–53.

[10] Ferrini F, Trang T, Mattioli TAM, Laffray S, Del'Guidice T, Lorenzo LE, Castonguay A, Doyon N, Zhang WB, Godin AG, Mohr D, Beggs S, Vandal K, Beaulieu JM, Cahill CM, Salter MW, De Koninck Y. Morphine

hyperalgesia gated through microglia-mediated disruption of neuronal Cl− homeostasis. Nat Neurosci 2013;16:183–92.

[11] Figurov A, PozzoMiller LD, Olafsson P, Wang T, Lu B. Regulation of synaptic responses to high-frequency stimulation and LTP by neurotrophins in the hippocampus. Nature 1996;381:706–9.

[12] Gomes C, Ferreira R, George J, Sanches R, Rodrigues DI, Goncalves N, Cunha RA. Activation of microglial cells triggers a release of brain-derived neurotrophic factor (BDNF) inducing their proliferation in an adenosine A2A receptor-dependent manner: a2A receptor blockade prevents BDNF release and proliferation of microglia. J Neuroinflammation 2013; 10:16.

[13] Groenewegen HJ. Organization of the afferent connections of the mediodorsal thalamic nucleus in the rat, related to the mediodorsal-prefrontal topography. Neuroscience 1988;24:379–431.

[14] Groth R, Aanonsen L. Spinal brain-derived neurotrophic factor (BDNF) produces hyperalgesia in normal mice while antisense directed against either BDNF or trkB, prevent inflammation-induced hyperalgesia. PAIN 2002;100:171–81.

[15] Hartman R, Lekic T, Rojas H, Tang JP, Zhang JH. Assessing functional outcomes following intracerebral hemorrhage in rats. Brain Res 2009; 1280:148–57.

[16] Head H, Holmes G. Sensory disturbances from cerebral lesions. Brain 1911;34:102–254.

[17] Hughes JP, Chessell I, Malamut R, Perkins M, Backonja M, Baron R, Farrar JT, Field MJ, Gereau RW, Gilron I, McMahon SB, Porreca F, Rappaport BA, Rice F, Richman LK, Segerdahl M, Seminowicz DA, Watkins LR, Waxman SG, Wiech K, Woolf C. Understanding chronic inflammatory and neuropathic pain. Ann N Y Acad Sci 2012;1255:30–44.

[18] Ji YY, Lu Y, Yang F, Shen WH, Tang TTT, Feng LY, Duan SM, Lu B. Acute and gradual increases in BDNF concentration elicit distinct signaling and functions in neurons. Nat Neurosci 2010;13:302–307.

[19] Jolivalt CG, Lee CA, Ramos KM, Calcutt NA. Allodynia and hyperalgesia in diabetic rats are mediated by GABA and depletion of spinal potassium-chloride co-transporters. PAIN 2008;140:48–57.

[20] Kahle KT, Staley KJ, Nahed BV, Gamba G, Hebert SC, Lifton RP, Mount DB. Roles of the cation-chloride cotransporters in neurological disease. Nat Clin Pract Neuro 2008;4:490–503.

[21] Kang HJ, Schuman EM. Long-lasting neurotrophin-induced enhancement of synaptic transmission in the adult hippocampus. Science 1995;267:1658–62.

[22] Kuan YH, Shih HC, Lu HC, Tang SC, Jeng JS, Shyu BC. Animal models of central post-stroke pain. PAIN 2015;2.

[23] Kuan YH, Shih HC, Tang SC, Jeng JS, Shyu BC. Animal models of central post-stroke pain. Recent Devel. Pain Res. India; Research Signpost, 2015;2:1–18.

[24] Kumar B, Kalita J, Kumar G, Misra UK. Central poststroke pain: a review of pathophysiology and treatment. Anesth Analgesia 2009;108:1645–57.

[25] Kumar G, Soni CR. Central post-stroke pain: current evidence. J Neurol Sci 2009;284:10–17.

[26] Llinas RR, Ribary U, Jeanmonod D, Kronberg E, Mitra PP. Thalamocortical dysrhythmia: a neurological and neuropsychiatric syndrome characterized by magnetoencephalography. Proc Natl Acad Sci U S A 1999;96:15222–7.

[27] Lu HC, Chang WJ, Kuan YH, Huang AC, Shyu BC. A [14C]iodoantipyrine study of inter-regional correlations of neural substrates following central post-stroke pain in rats. Mol Pain 2015;11:9.

[28] Marchand F, Perretti M, McMahon SB. Role of the immune system in chronic pain. Nat Rev Neurosci 2005;6:521–32.

[29] Misra UK, Kalita J, Kumar B. A study of clinical, magnetic resonance imaging, and somatosensory-evoked potential in central post-stroke pain. J Pain 2008;9:1116–22.

[30] Mol BrainBroderick J, Connolly S, Feldmann E, Hanley D, Kase C, Krieger D, Mayberg M, Morgenstern L, Ogilvy CS, Vespa P, Zuccarello M; American Heart Association/American Stroke Association Stroke C, American Heart Association/American Stroke Association High Blood Pressure Research C, Quality of C, Outcomes in Research Interdisciplinary Working G. Guidelines for the management of spontaneous intracerebral hemorrhage in adults: 2007 update: a guideline from the american heart association/american stroke association stroke council, high blood pressure research council, and the quality of care and outcomes in research interdisciplinary working group. Circulation 2007;116:e391–413.

[31] Myers RR, Campana WM, Shubayev VI. The role of neuroinflammation in neuropathic pain: mechanisms and therapeutic targets. Drug Discov Today 2006;11:8–20.

[32] Scholz J, Woolf CJ. The neuropathic pain triad: neurons, immune cells and glia. Nat Neurosci 2007;10:1361–8.

[33] Stefani LC, Torres ILD, de Souza ICC, Rozisky JR, Fregni F, Caumo W. BDNF as an effect modifier for gender effects on pain thresholds in healthy subjects. Neurosci Lett 2012;514:62–6.

[34] Trang T, Beggs S, Wan X, Salter MW. P2X4-receptor-mediated synthesis and release of brain-derived neurotrophic factor in microglia is dependent on calcium and p38-mitogen-activated protein kinase activation. J Neurosci 2009;29:3518–28.

[35] Wang GX, Thompson SM. Maladaptive homeostatic plasticity in a rodent model of central pain syndrome: thalamic hyperexcitability after spinothalamic tract lesions. J Neurosci 2008;28:11959–69.

[36] Wasserman JK, Koeberle PD. Development and characterization of a hemorrhagic rat model of central post-stroke pain. Neuroscience 2009; 161:173–83.

[37] Yajima Y, Narita M, Usui A, Kaneko C, Miyatake M, Narita M, Yamaguchi T, Tamaki H, Wachi H, Seyama Y, Suzuki T. Direct evidence for the involvement of brain-derived neurotrophic factor in the development of a neuropathic pain-like state in mice. J Neurochem 2005;93:584–94.

[38] Yezierski RP. Spinal cord injury: a model of central neuropathic pain. Neuro-Signals 2005;14:182–93.

[39] Zhang X, Wang J, Zhou Q, Xu Y, Pu S, Wu J, Xue Y, Tian Y, Lu J, Jiang W, Du D. Brain-derived neurotrophic factor-activated astrocytes produce mechanical allodynia in neuropathic pain. Neuroscience 2011;199:452–60.

[40] Zhang X, Zeng LL, Yu TT, Xu YM, Pu SF, Du DP, Jiang W. Positive feedback loop of autocrine BDNF from microglia causes prolonged microglia activation. Cell Physiol Biochem 2014;34:715–23.

[41] Zhu ZW, Friess H, Wang L, Zimmermann A, Buchler MW. Brain-derived neurotrophic factor (BDNF) is upregulated and associated with pain in chronic pancreatitis. Dig Dis Sci 2001;46:1633–9.

[42] Zhuo M, Wu G, Wu LJ. Neuronal and microglial mechanisms of neuropathic pain. Mol Brain 2011;4:31.